Supporting Information

On the structural stability of crystalline ceria phases in undoped and acceptor-doped ceria materials under *in situ* reduction conditions

Maged F. Bekheet,[‡] Matthias Grünbacher,[†] Lukas Schlicker,[‡] Albert Gili[‡], Andrew Doran[#], Jan Dirk Epping,[ǁ] Aleksander Gurlo,[‡] Bernhard Klötzer,[†] Simon Penner*[,†]

[‡] *Fachgebiet Keramische Werkstoffe/ Chair of Advanced Ceramic Materials, Institut für Werkstoffwissenschaften und -technologien, Technische Universität Berlin, Hardenbergstr. 40, 10623 Berlin, Germany*

[†] *Institute of Physical Chemistry, University of Innsbruck, Innrain 52c, A-6020 Innsbruck*

[#] *Advanced Light Source, Lawrence Berkeley National Laboratory Berkeley, California 94720, USA*

[ǁ] *Fakultät II : Mathematik & Naturwissenschaften, Institut für Chemie, Technische Universität Berlin, Hardenbergstr. 40, 10623 Berlin, Germany*

Keywords: *in situ*, rhombohedral Ce_7O_{12}, triclinic $Ce_{11}O_{20}$, X-ray diffraction, hydrogen reduction, bixbyite

*Corresponding author: Simon Penner, simon.penner@uibk.ac.at, Tel: +43 512 507 58003

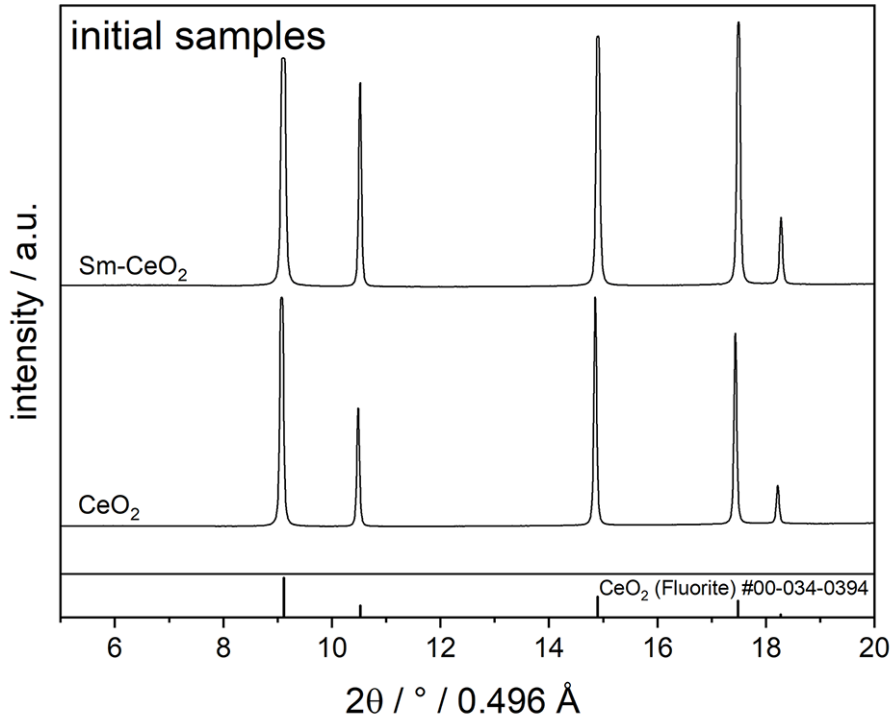

Figure S1: X-ray diffraction patterns of the initial ceria materials, corroborating the presence of fluorite-type CeO_2.

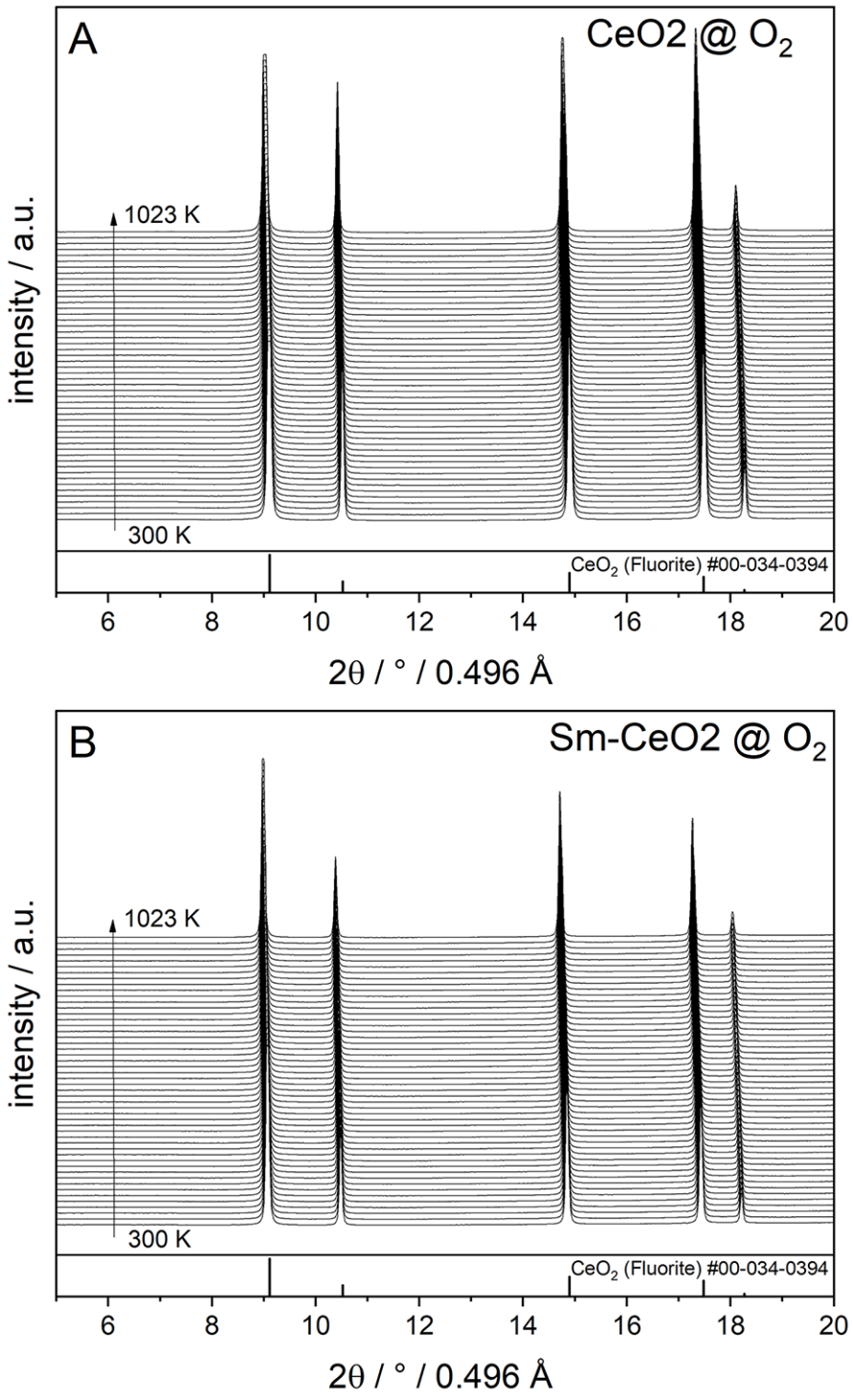

Figure S2: Temperature-dependent *in situ* X-ray diffractograms of pure and Sm-doped CeO_2 collected during calcination in oxygen up to 1023 K.

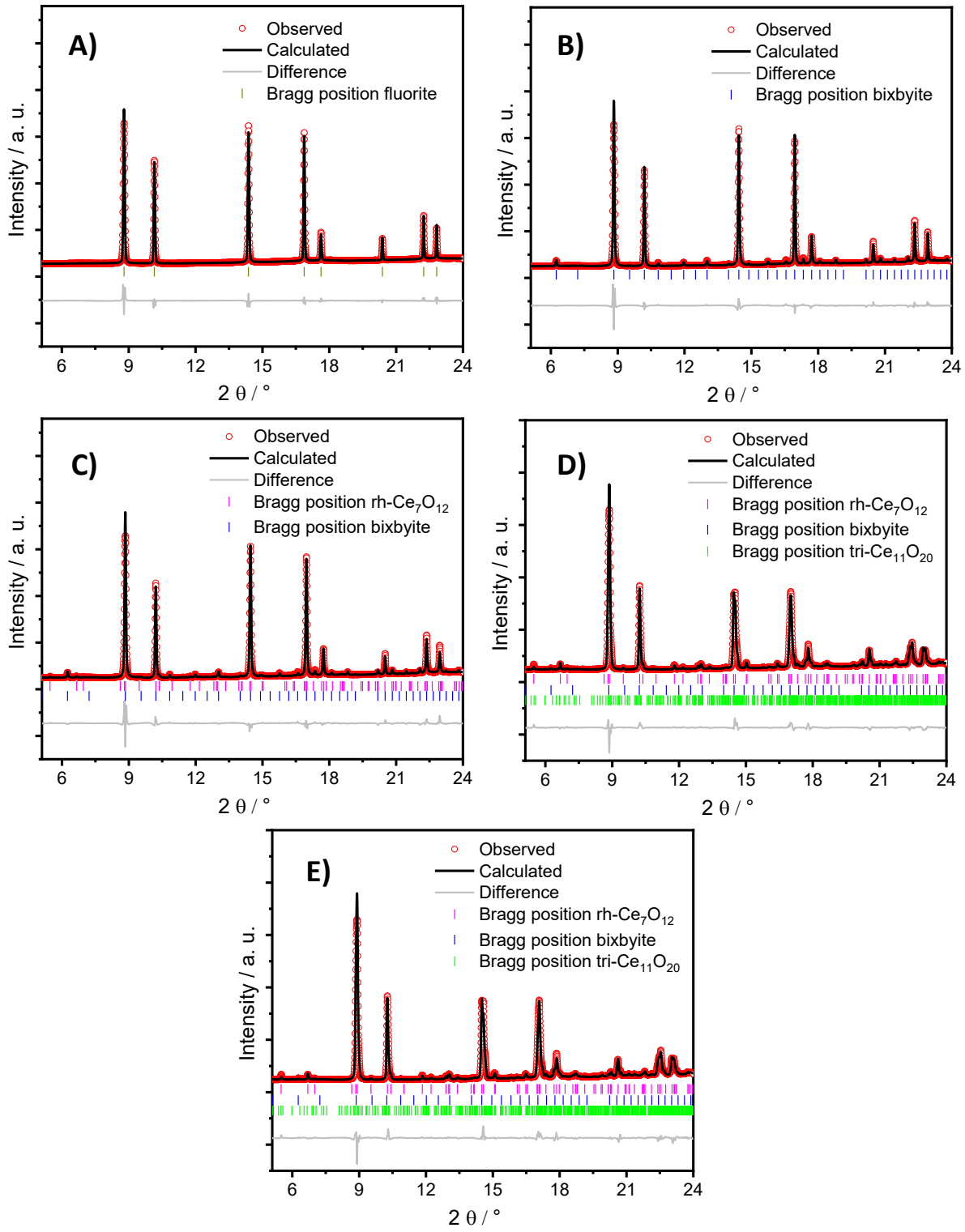

Figure S3: Structure refinement of X-ray powder diffraction data collected at 1273 K (A), 1000 K (B), 900 K (C), 600 K (D) and 300 K (E) for pure CeO_2 sample during cooling from 1273 K in H_2 atmosphere showing the observed (red circle) and calculated (black solid line) intensities, the calculated Bragg reflections (tick marks), and the difference (gray solid line).

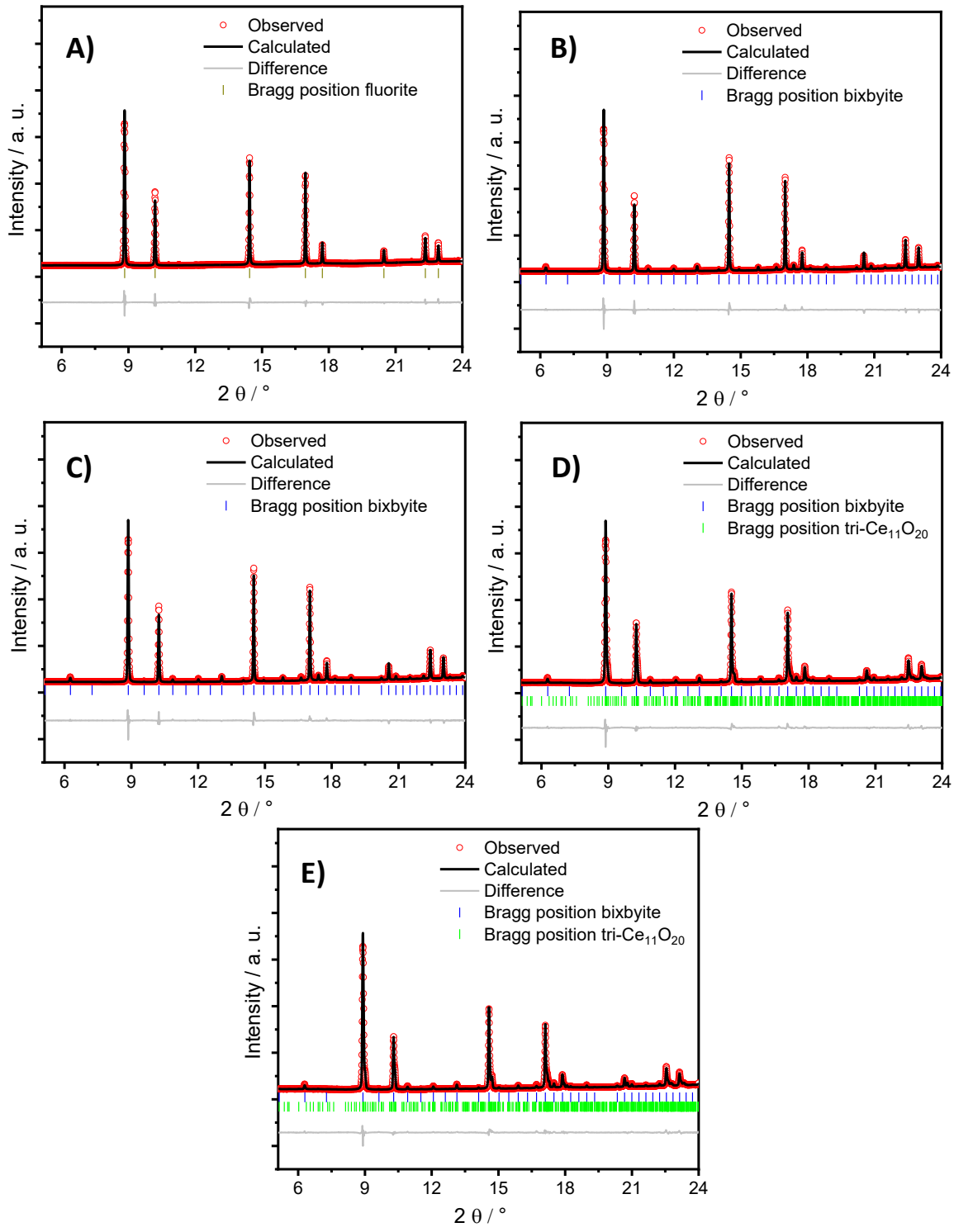

Figure S4: Structure refinement of X-ray powder diffraction data collected at 1273 K (A), 1000 K (B), 900 K (C), 600 K (D) and 300 K (E) for SDC15 sample during cooling from 1273 K in H_2 atmosphere showing the observed (red circle) and calculated (black solid line) intensities, the calculated Bragg reflections (tick marks), and the difference (gray solid line).

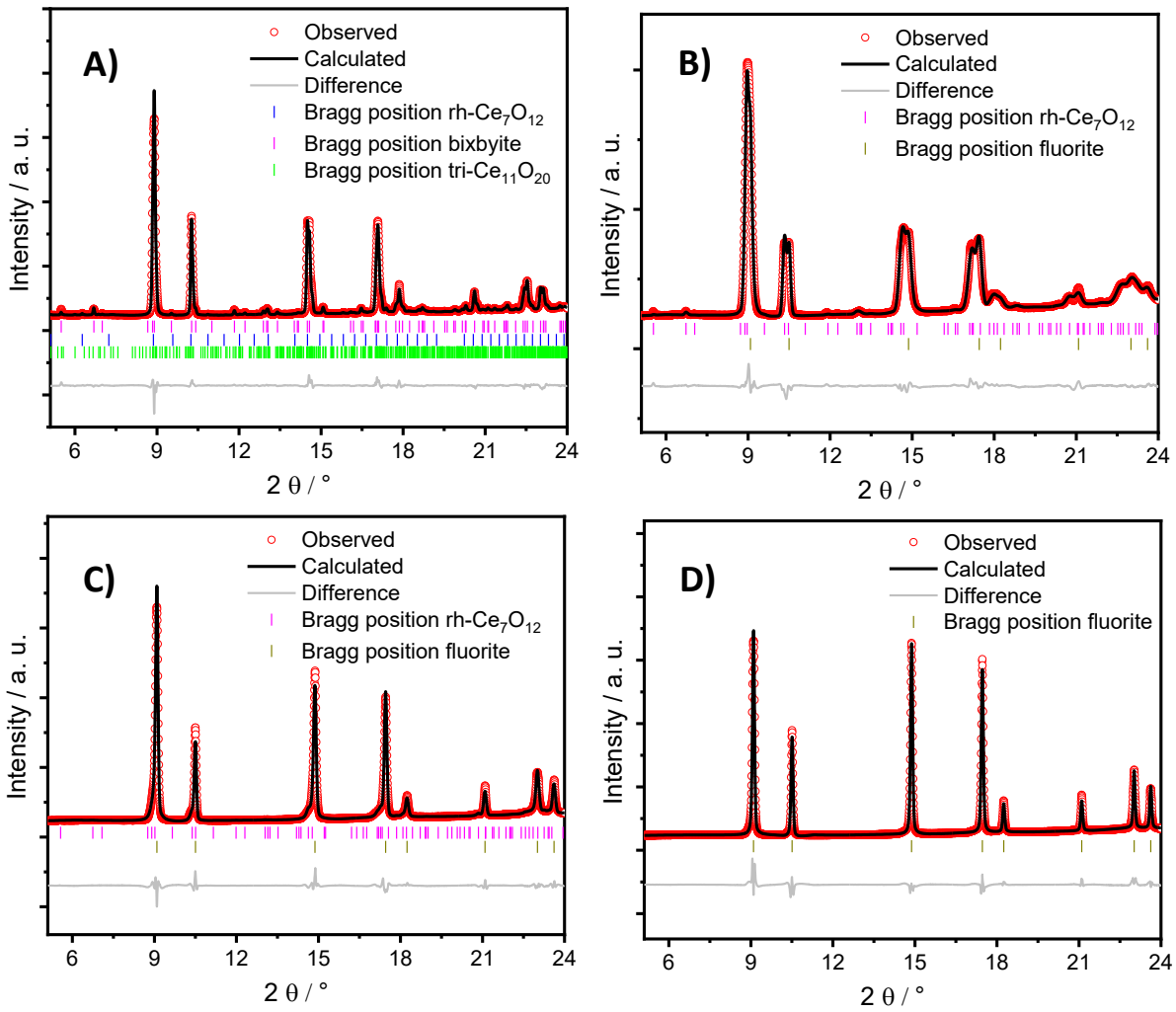

Figure S5: Structure refinement of X-ray powder diffraction data collected at 300 K (A), 345 K (B), 375 K (C) and 400 K (D) for pure CeO_2 sample during re-oxidation in flowing O_2 atmosphere showing the observed (red circle) and calculated (black solid line) intensities, the calculated Bragg reflections (tick marks), and the difference (gray solid line).

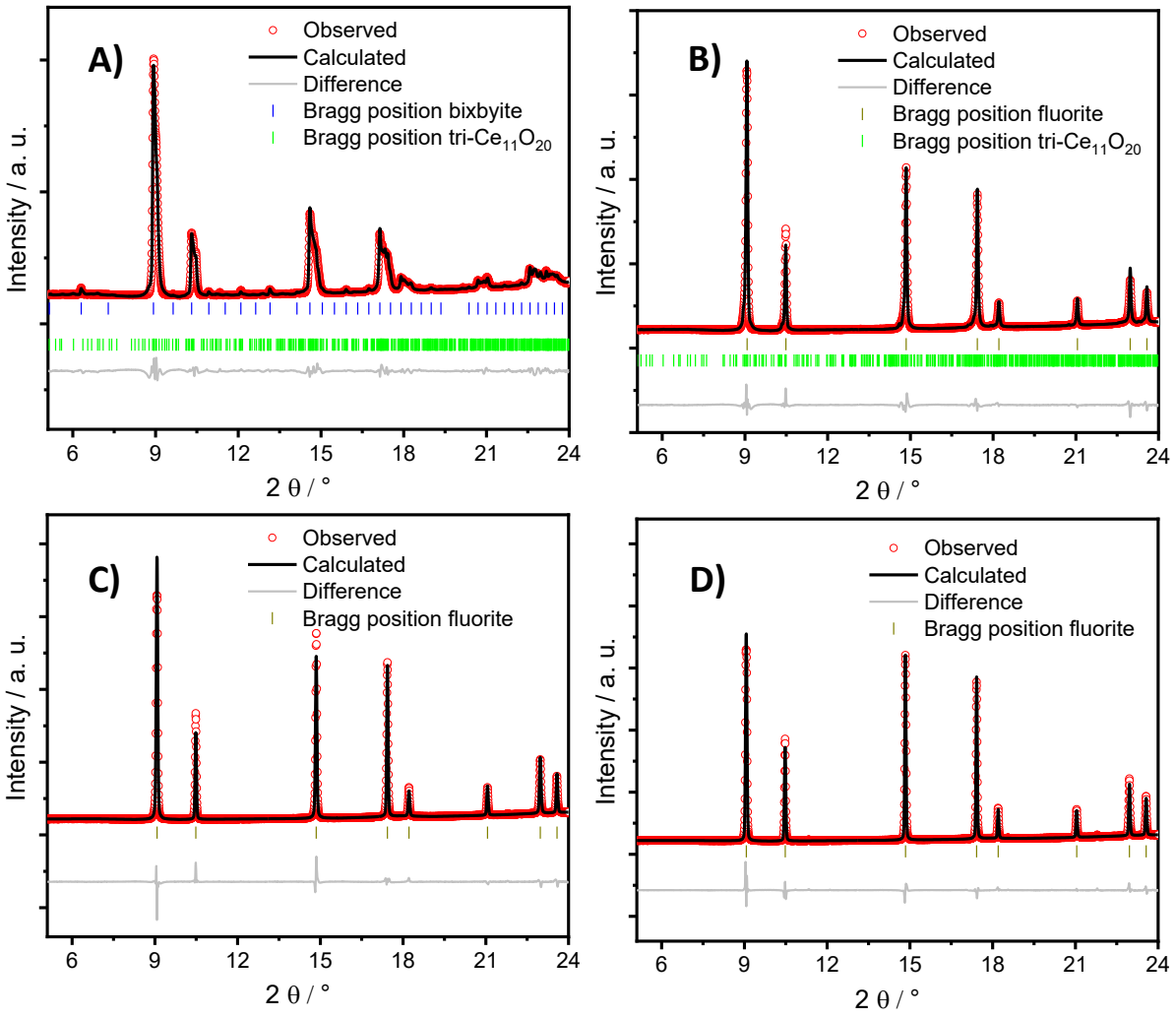

Figure S6: Structure refinement of X-ray powder diffraction data collected at 300 K (A), 330 K (B), 345 K (C) and 400 K (D) for SDC15 sample during re-oxidation in flowing O_2 atmosphere showing the observed (red circle) and calculated (black solid line) intensities, the calculated Bragg reflections (tick marks), and the difference (gray solid line).

Table S1: A summary of information extracted from XRD patterns by Rietveld refinement of CeO_2 sample after reduction and during cooling in the flowing H_2 atmosphere showing weight fraction wt. [%], lattice parameters a, b, c [Å], the unit cell volume V [$Å^3$], lattice angles α, β, γ [°], oxygen vacancy parameter δ and mole fraction y of Ce^{3+}. The values of oxygen vacancy parameter δ and mole fraction y of Ce^{3+} are calculated according to the relationship between the amount of oxygen (i.e. 2-δ) in $CeO_{2-\delta}$ and the pseudo-cubic lattice parameters a, as well as using equation 2 (i.e. are given in square brackets).

Temp. (K)	**Cubic fluorite** ($Fm\bar{3}m$, Z = 4)	**Cubic bixbyite** ($I\bar{3}a$, Z = 16)	**rh-Ce_7O_{12}** ($R\bar{3}$, Z = 3)	**tri-$Ce_{11}O_{20}$** ($P\bar{1}$, Z = 1)
1273	wt.% = 100 a = 5.60423(1) V = 176.02(1) δ = 0.29 [0.23] y = 0.58 [0.46]	-	-	-
1000	-	wt.% = 100 a = 11.1659(4) V = 1392.14(1) δ = 0.29 y = 0.58	-	-
900	-	wt.% = 96.4(8) a = 11.1503(7) V = 1386.31(1) δ = 0.29 y = 0.58	wt.% = 3.6(7) a = 10.4121(7) c = 9.6789(8) V = 908.73(9) δ = 0.29 y = 0.58	-
600	-	wt.% = 11.4(7) a = 11.1348(3) V = 1380.55(6) δ = 0.31 y = 0.62	wt.% = 66.0(9) a = 10.3738(1) c = 9.6820(1) V = 902.34(2) δ = 0.30 y = 0.60	wt.% = 22.6(4) a = 6.8432(4) b = 10.3075(4) c = 6.7486(3) α = 89.75(4) β = 99.83(3) γ = 96.23(5) V = 466.21(4) δ = 0.24 y = 0.48
300	-	wt.% = 12.1(7) a = 11.1088(3) V = 1370.78(8) δ = 0.33 y = 0.66	wt.% = 62.4(8) a = 10.3410(1) c = 9.6493(1) V = 893.62(2) δ = 0.30 y = 0.60	wt.% = 25.5(6) a = 6.8057(4) b = 10.2830(5) c = 6.7314(3) α = 89.74(4) β = 99.82(3) γ = 96.21(5) V = 461.41(4) δ = 0.24 y = 0.48

Table S2: A summary of information extracted from XRD patterns by Rietveld refinement of SDC15 sample after reduction and during cooling in the flowing H_2 atmosphere showing weight fraction wt. [%], lattice parameters a, b, c [Å], the unit cell volume V [Å^3], lattice angles α, β, γ [°], oxygen vacancy parameter δ and mole fraction y of Ce^{3+}. The values of oxygen vacancy parameter δ and mole fraction y of Ce^{3+} are calculated according to the relationship between the amount of oxygen (*i.e.* 2-δ) in $CeO_{2-\delta}$ and the pseudo-cubic lattice parameters a, as well as using equation 2 (i.e. are given in square brackets).

Temp. (K)	**Cubic fluorite** ($Fm\bar{3}m$, Z = 4)	**Cubic bixbyite** ($I\bar{3}a$, Z = 16)	**tri-$Ce_{11}O_{20}$** ($P\bar{1}$, Z = 1)
1273	wt.% = 100 a = 5.58182(2) V = 173.91(1) δ = 0.27 [0.23] y = 0.39 [0.31]	-	-
1000	-	wt.% = 100 a = 11.11621(2) V = 1373.63(1) δ = 0.27 y = 0.39	-
900	-	83.5(8)% a = 11.08875(3) V = 1363.48(1) δ = 0.29 y = 0.43	-
600	-	wt.% = 11.4(7) a = 11.1348(3) V = 1380.55(6) δ = 0.31 y = 0.47	wt.% = 16.5(4) a = 6.77(2) b = 10.2629(3) c = 6.7698(3) α = 90.06(4) β = 99.66(3) γ = 96.01(5) V = 461.65(3) δ = 0.23 y = 0.31
300	-	wt.% = 78.8(7) a = 11.05818(3) V = 1352.23(6) δ = 0.31 y = 0.47	wt.% = 21.2(6) a = 6.7573(2) b = 10.2264(2) c = 6.7466(2) α = 90.09(2) β = 99.64(3) γ = 95.92(2) V = 457.09(2) δ = 0.23 y = 0.31